ACS OMEGA

http://pubs.acs.org/journal/acsodf

Article

Mineral and Technological Features of Magnetite–Hematite Ores and Their Influence on the Choice of Processing Technology

Nadezhda V. Nikolaeva,* Tatiana N. Aleksandrova, Elena L. Chanturiya, and Anastasia Afanasova

Cite This: *ACS Omega* 2021, 6, 9077–9085

Read Online

ACCESS | Metrics & More | Article Recommendations

ABSTRACT: Analysis of the current technical solutions for the processing of iron ores showed that the high-grade ores are directly exposed to metallurgical processing; by comparison, low-grade ores, depending on the mineralogical and material composition, are directed to beneficiation including gravitational, magnetic, and flotation processes or their combination. Obtaining high-quality concentrates with high iron content and low content of impurities from low-grade iron ores requires the maximum possible liberation of valuable minerals and a high accuracy of separating features (difference in density, magnetic susceptibility, wettability, etc.). Mineralogical studies have established that the main iron-bearing mineral is hematite, which contains 69.02 to 70.35% of iron distributed in the ore. Magnetite and hydrogoethite account for 16.71−17.74 and 8.04−10.50% of the component, respectively; the proportion of iron distributed in gangue minerals and finely dispersed iron hydroxides is very insignificant. Iron is mainly present in the trivalent form—Fe_2O_3 content ranges from 50.69 to 51.88%; bivalent iron is present in small quantities—the FeO content in the samples ranges from 3.53 to 4.16%. The content of magnetic iron is 11.40−12.67%. Based on the obtained results by the investigation of the features of magnetite−hematite ores from the Mikhailovskoye deposit, a technological scheme of magneto-flotation beneficiation was proposed, which allows producing iron concentrates with 69% of iron content and less than 2.7% silicon dioxide for the production of pellets with subsequent metallization.

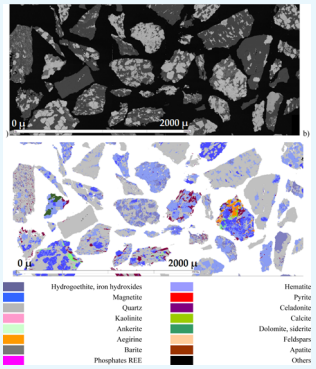

INTRODUCTION

Depletion of the mineral ore base of high-grade quality and easily beneficiated iron ores has led to the need for improvement in the processing of low-grade and complex composition magnetite−hematite ores. This, in turn, has led to the complication of technological schemes used in their processing.[1−7] Analysis of the current technical solutions for the processing of iron ores showed that the high-grade ores are directly exposed to metallurgical processing. However, low-grade ores depending on mineralogical and material composition are directed to beneficiation including gravitational, magnetic, and flotation processes or their combination.[8−15] The search for new technologies and improvement of existing technologies for the processing of iron-containing mineral raw materials will make it possible to compensate for the decrease in the quality of the mineral resource base of iron ores by involving complex and low-quality raw materials in the processing.[16−18]

Unfavorable factors affecting beneficiation of low-grade magnetite−hematite ores, including oxidized ferruginous quartzite, are widespread development of complex intergrowths of magnetite and hematite, making it difficult to separate these minerals; development of a marked proportion of dispersed hematite and fine hematite in quartz, siderite, and green mica; the presence of many very thin residuals, relic inclusions of magnetite in hematite, and incipient complex filamentary hematite inclusions in magnetite; and the presence in the ore in appreciable amounts of high-iron green hydromica, which reduces beneficiation parameters.[19]

Obtaining high-quality concentrates with high iron content and low content of impurities from low-grade iron ores requires the maximum possible liberation of valuable minerals and high accuracy of separating features (difference in density, magnetic susceptibility, wettability, etc.). One of the upcoming trends in the processing of iron-bearing ores from the technological point is regrinding and flotation repreparation of iron ore concentrates obtained after magnetic separation.[8−15,17,18] An actual trend for the investigation of flotation of iron ores is the selection of reagent regimes.[20−22] Starch, carboxymethyl cellulose, and lignosulphonates are the most used as depressant reagents.[23−25] Ether amines are by far the most utilized class of collector.[26,27]

A striking example of low-grade magnetite−hematite ores is the Mikhailovskoye deposit. The magnetite−hematite ores of the Mikhailovskoye deposit are characterized by fine dissemination of ore and gangue minerals, the complexity of

Received: January 8, 2021
Accepted: March 15, 2021
Published: March 24, 2021

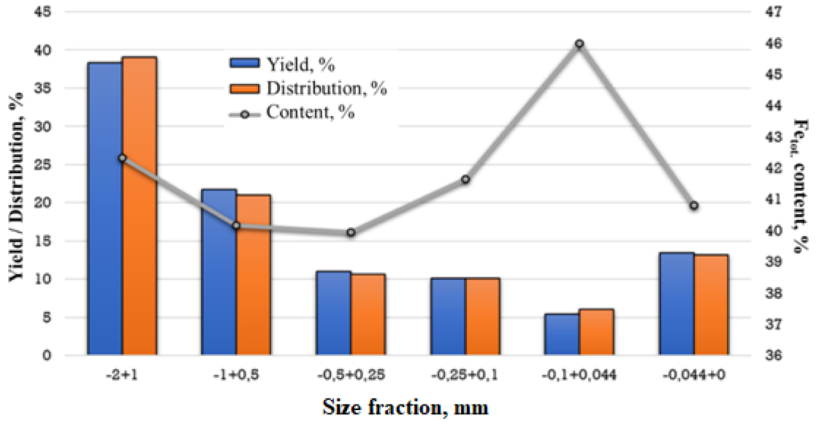

Figure 1. Histogram of the yield of classes and the content and distribution of total iron in the size classes.

the structural and textural features and material composition, a low-level contrast in the magnetic properties of the separated minerals, and so forth.[28−30] The content of iron in these ores ranges from 38.3 to 40.1%, the average content of silica is in the range of 39.10 to 41.80%, which classifies the iron ore as a "low-Fe grade". The reserves of these magnetite−hematite ores are significant and amount to about 2.2 billion tons. Currently, these ores are not being beneficiated due to the lack of a cost-effective processing technology, which is primarily caused by the limited knowledge available.

At present, various studies are conducted to increase the integrated approach of the use of the raw material base of the Mikhailovskoye deposit in the development of combined technological schemes.[31−35] However, detailed systematic work on the study of quality and distribution of valuable components and their impact on beneficiation has not been carried out. The purpose of this work was to find optimal technological solutions to improve the quality of iron ore concentrates in beneficiation of magnetite-hematite ores of the Mikhailovskoye deposit using a comprehensive approach to the study of material, chemical, and phase composition.

RESULTS AND DISCUSSION

Features of the Material Composition. Analysis of particle size distribution of the material size of 2 mm followed by chemical analysis (Figure 1) was conducted to study the distribution of the analyzed components by size classes. The main valuable component is iron, the content of which ranges from 38.8 to 39.49% Fe. Iron is mainly present in the trivalent form—Fe_2O_3 content ranges from 50.69 to 51.88%; bivalent iron is present in small quantities—the FeO content in the samples ranges from 3.53 to 4.16%. The content of magnetic iron is 11.40−12.67%. Impurities in the ore are represented by phosphorus and sulfur. For the studied ore, the presence of phosphorus can be noted. The content of phosphorus pentoxide was 0.14%. The sulfur content is in the range of 0.02−0.04%.

The distribution of the total iron content in all size classes is fairly uniform and varies in the range of 39.95% in the class −0.5 + 0.25 mm to 45.98% in the class −0.1 + 0.044 mm (with a difference in absolute terms of 6.03%) with an initial content of 41.52%. Analysis of the distribution of magnetite iron showed that in the class −2 + 1 mm, the minimum value was noted. The content of silicon oxide in the samples has close values and is about 43%; with a maximum value of 45.03% in the class −1 + 0.5 mm.

For analysis, a representative sample weighing 100 mg was taken from the total sample. Mossbauer spectra were processed using the Univem MS program. The Mossbauer spectra of the source material are shown in Figure 2.

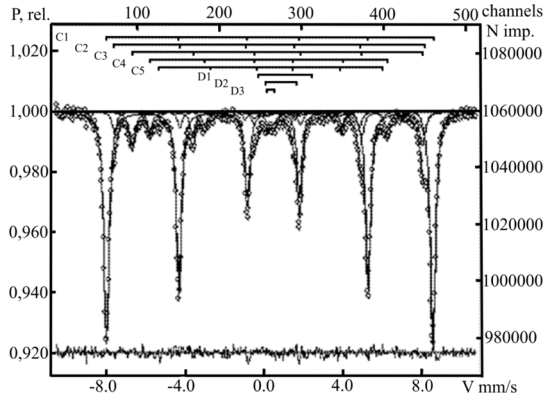

Figure 2. Mossbauer spectra.

Sextets belong to hematite, magnetite, and hydrogoethite. Sextet C1 corresponds to the octahedral position of the ferric iron of hematite. Sextet C2 is due to Fe^{3+} ions of the tetrahedral position in the magnetite lattice, while sextet C3 is due to ions of the octahedral position. The area ratio of tetrahedral and octahedral iron ions in the spectrum differs from 0.5 of stoichiometric magnetite, which indicates isomorphic impurities in its lattice. Sextets C4 and C5 correspond to the octahedral position of ferric hydrogoethite.

Doublets belong to silicate and carbonate ferrous phases, as well as finely dispersed iron hydroxides. The interpretation of sextets, doublets, and the corresponding distribution of iron over valence states are given in Table 1.

It has been found that the main iron-bearing mineral is hematite, which contains 69.02 to 70.35% of iron distributed in the ore. Magnetite and hydrogoethite account for 16.71−17.74 and 8.04−10.50% of the component, respectively; the proportion of iron distributed in gangue minerals and finely dispersed iron hydroxides is very insignificant. Thus, the main iron losses during magnetic separation are accounted for by hematite and hydrogoethite, which have a very low magnetic susceptibility.

The average mineral composition of a sample of the magnetite−hematite ore, determined by taking into account the data of optical and electron microscopic studies, local X-ray

https://doi.org/10.1021/acsomega.1c00129
ACS Omega 2021, 6, 9077−9085

Table 1. Mossbauer Parameters

spectrum component	isomeric shift δ, mm/s	quadrupole splitting Δ, mm/s	magnetic fields on nuclei $Fe^{57}H$, kE	cmponent areas S, %	interpretation
C1(Fe3+)VI	0.3703	−0.1894	514.68	70.35	hematite
C2(Fe3+)IV	0.2781	−0.0125	488.86	5.97	magnetite
C3(Fe2++Fe3+) VI	0.6667	067	457.24	11.77	
C4(Fe3+)VI	0.3564	−0.2230	374.22	5.93	hydrogoethite
C5(Fe3+)VI	0.4373	−0.2196	351.98	2.11	
D1(Fe2+)VI	1.0294	2.7423		0.66	Fe^{2+}silicate, carbonate
D2(Fe3+)VI	0.8521	1.5885		1.55	Fe^{3+}silicate
D3(Fe3+)VI	0.3245	0.3317		1.68	finely dispersed Fe oxides and silicates

spectral and chemical analyzes, and Mossbauer spectroscopy, is given in Table 2.

Table 2. Mineral Composition

mineral	content, %
quartz	40.58
hematite, martite	36.96
magnetite	9.59
hydrogoethite	3.96
iron hydroxides	0.94
pyrite	0.04
celadonite	3.31
kaolinite	1.55
carbonates (siderite, ankerite)	1.67
REE phosphates	0.56
barite	0.20
aegirine	0.64
amount	**100.00**

Thus, it has been established that the predominant minerals in the ore are quartz, iron oxides, and hydroxides, the fluctuations in the content of which according to the samples are insignificant: quartz—40.58% and iron oxides and hydroxides—52.54%.

Based on the data of microscopical analysis, it was established that ferruginous quartzites are characterized by a thin-striped layered texture, in which the thick quartz-bearing layers, differing in the content of iron oxide minerals, are small and range up to 2−3 mm (Figure 3). The structure of the rocks is microgranoblastic.

The main ore minerals in the studied ore are hematite, magnetite, and hydrogoethite; finely dispersed iron hydroxides and, in isolated cases, pyrite are noted in much smaller amounts. The predominant mineral oxide is hematite, formed by replacing ferrous components of magnetite quartzite. The degree of replacement of magnetite is different, including up to complete pseudomorphs of hematite over magnetite. Interlayers with partially replaced (up to 50−70% of the grain area) magnetite are quite often noted. Magnetite in the form of separate relict particles is present in the hematite matrix in the form of closed intergrowths. As a result of magnetic separation, magnetite is recovered into the tailings (Figures 4 and 5).

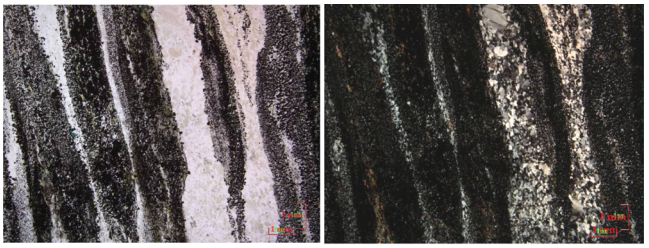

a) b)

Figure 3. Micrograph of the magnetite−hematite ore with (a) one nicol and (b) crossed nicol prisms.

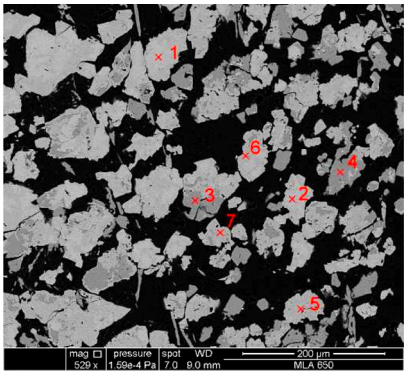

Figure 4. Hematite intergrowth with magnetite and hydrogoethite in polyhedral grain aggregates.

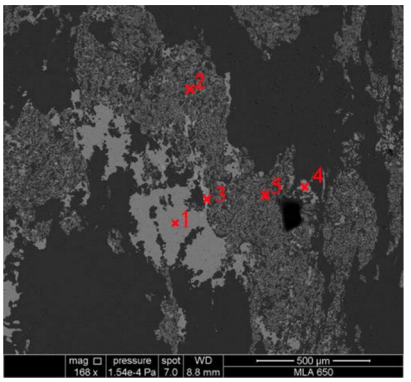

Figure 5. Clusters of iron hydroxides highlighting the microfolding of ferruginous quartzites.

Along with closed intergrowths of magnetite, open intergrowths are visualized in the hematite matrix, which, upon magnetic separation, will precipitate into magnetite concentrates, which will lead to a decrease in the iron content in it. In separate layers, in a close intergrowth with hematite and magnetite, hydrogoethite is visualized, the ingress of which into

https://doi.org/10.1021/acsomega.1c00129
ACS Omega 2021, 6, 9077−9085

Table 3. Chemical Composition of Iron Oxides and Hydroxides

	content, %							
no.	Fe	Si	Al	Mg	P	O	amount	notice
				Magnetite				
1	70.76	0.56				28.68	100.00	Figure 5, spectrum 1
2	69.44	1.39				29.17	100.00	Figure 5, spectrum 2
				Hematite				
3	68.51	0.58				30.91	100.00	Figure 5, spectrum 5
4	66.93	1.07				32.01	100.01	Figure 5, spectrum 6
				Iron Hydroxides (Hydrogoethite)				
5	56.40	0.96	0.94			41.70	100.00	Figure 5, spectrum 3
6	51.93	3.33	0.91			43.83	100.00	Figure 5, spectrum 4
7	58.25	1.27	0.37	0.24	0.24	39.63	100.00	Figure 6, spectrum 4
				Finely Dispersed Aggregates of Iron Hydroxides in Quartz				
8	31.99	21.52				46.49	100.00	Figure 6, spectrum 2
9	25.93	26.41				47.66	100.00	Figure 6, spectrum 5

Table 4. Mineral Composition of Classified Material According to MLA Data

	content, %						
mineral	−2 + 1 mm	−1 + 0.5 mm	−0.5 + 0.25 mm	−0.25 + 0.1 mm	−0.1 + 0.044 mm	−0.044 + 0 mm	feed ore (by balance)
hematite	39.69	37.25	39.12	38.92	43.33	35.73	38.70
magnetite	13.15	17.03	11.15	13.39	13.48	8.09	13.13
hydrogoethite	6.20	5.40	5.49	5.01	6.38	14.82	6.99
quartz	37.23	36.56	40.08	37.95	32.22	31.29	36.40
celadonite	2.27	2.35	2.10	2.24	2.67	7.05	2.93
carbonate	1.05	0.99	1.27	1.37	1.06	1.33	1.13
other minerals	0.41	0.42	0.79	1.12	0.86	1.69	0.72
amount	100.00	100.00	100.00	100.00	100.00	100.00	100.00

the magnetite concentrate will lead to an even greater decrease in its iron content.

The content of hematite in individual layers varies from 10 to 70%. The predominant form of mineral segregations into interlayers with a content of up to 40% is fine dissemination with a particle size of 5−35 μm both in the intergranular space of quartz grains and within them. Coarser grains of hematite form continuous and band-like aggregates, often with an abundance of microinclusions of gangue minerals.

The extremely small size of hematite segregations and thin intergrowths with quartz can lead to incomplete liberation of hematite during its grinding and, as a consequence, to the concentration of the mineral in the tailings, and micro-inclusions of gangue minerals in hematite can significantly reduce the quality of the hematite concentrate.

The chemical composition of hematite, determined by local X-ray spectral analysis, is given in Table 3. The iron content in the mineral ranges from 64.92 to 68.55% with an average value of 66.39%, which is 5.16% rel. less than the theoretical value. An impurity in the composition of hematite is silicon, the average content of which is 0.42%, which in terms of silicon oxide will be 0.9%. In the chemical composition of hydrogoethite, the iron content ranges from 51.93 to 62.78% with an average value of 58.11%. The presence of intergrowths of hydrogoethite with hematite and magnetite in ores can significantly reduce the iron content in the concentrate during gravity and flotation beneficiation methods.

Iron hydroxides are present in the microquartzite matrix mainly in a finely dispersed form, as a result of which the interlayers of microquartzites acquire a brownish-reddish color. In the areas of microfolding of rocks, iron hydroxides are redistributed, forming thin interlayers and emphasizing the folding of rocks. The size of the precipitation of iron hydroxides does not allow determining the chemical composition of minerals; therefore, Table 4 shows the chemical composition of aggregates of iron hydroxides with quartz, in which the content of iron and silicon is 25.93−31.99 and 21.52−26.41%, respectively.

The step-by-step processing of the material during mineralogical analysis (MLA) is shown on a sample of the material of the size class −0.5 + 0.25 mm. In the original images of backscattered electrons (Figure 6a), according to the brightness characteristics, the mineral aggregate density which is higher than that of the background was distinguished. Simultaneous with scanning the surface, a step-by-step point X-ray spectral analysis of each mineral phase was carried out. Areas with the same brightness parameters and similar elemental composition were distinguished in a separate phase, colored with the same color. The resulting image of classified mineral aggregates, which was used for subsequent statistical processing, is shown in Figure 6b.

The mineral composition of the classified material of the samples after the grouping of minerals is given in Table 4.

It was found that the content of the predominant ore mineral—hematite in grain size classes over 0.1 mm varies slightly—from 37.25 to 39.69%. An increase in the content of hematite to 43.33% is noted in the size class of −0.1 + 0.044 mm, followed by a rather sharp decrease to 35.73% in the finest class, which indicates some liberation of hematite in the size class −0.1 + 0.044 mm. However, the content of hematite in the size class of −0.044 + 0 mm does not differ significantly from its content in the feed ore, which is an indirect sign of a weak liberation of the mineral even with the finest grinding

https://doi.org/10.1021/acsomega.1c00129
ACS Omega 2021, 6, 9077−9085

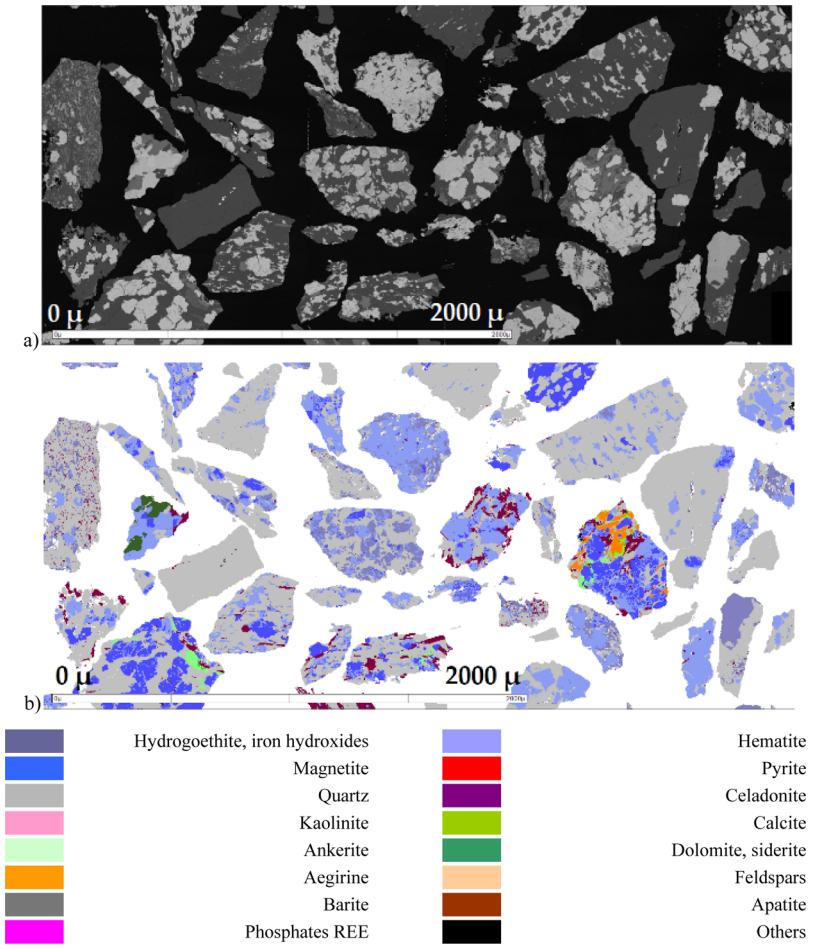

Figure 6. Initial image of magnetite−hematite ores with a particle size of −0.5 + 0.25 mm with backscattered electrons (a) and classified in accordance with the database (b).

(Table 5). In the size class −0.044 + 0 mm, only celadonite and hydrogoethite are significantly exposed.

The iron content in all size classes, except for the −0.1 + 0.044 mm class, changes insignificantly from 39.42 to 42.32%—in the −0.1 + 0.44 mm size class, it reaches 44.62%—and the average content of the component in the sample is 41.57%. The content of silicon, as well as iron, varies insignificantly in the size classes—from 15.90 to 19.41%—with an average content in the sample of 17.91%.

Ore minerals samples are oxides and hydroxides of iron−hematite, magnetite, and hydrogoethite. The iron distribution of minerals is given in Table 6.

The main Fe-bearing mineral in the samples is hematite, which contains 65.09% of the iron in the samples. The share of magnetite and hydrogoethite is 22.86 and 10.17% of iron, respectively. The amount of iron distribution in hematite and magnetite is the same—87.95%. The proportion of iron distributed to other phases is exceptionally low. It should be noted that the data of the automated MLA are in good agreement with the data of Moessbauer spectroscopy on the distribution of iron over minerals.

The automated MLA determined the size of the main ore iron-bearing minerals and the quality of the intergrowths, which include these minerals. The predominant grain size of magnetite grains is less than 0.25 mm (79.89%) and for hydrogoethite is less than 0.044 mm (55.03%). The size distribution of quartz particles is the opposite to that of hematite—particles with a particle size of more than 0.25 mm (64.70%) prevail, with a significant proportion of smaller particles. The distribution of minerals by size classes showed that in the finest class, the most liberate are the intergrowths containing hydrogoethite; the degree of liberation of the main ore minerals, hematite and magnetite, is rather low.

The summary data indicate the impossibility of obtaining a pure magnetite product even with the finest grinding of ore using the magnetic separation technology. As a result of magnetic separation, mainly high-grade and run-of-mine intergrowths of magnetite with hematite and quartz are extracted into the magnetite concentrate, which will lead to an increased content of silicon in the concentrate. It also notes a decrease in the iron content due to hematite since the iron content in hematite is lower than that in magnetite. Thus, analysis of aggregates containing essential mineral ores—quartz, hematite, magnetite, and hydrogoethite—showed all of these mineral phases forming an intimate fusion with each other, whereby even when the fine grinding ore degree liberation is very low, which allows us to classify them as very difficult to beneficiate according to classical beneficiation schemes.

Beneficiation of Magnetite−Hematite Ores. Studies have found that the ore contains both strongly magnetic and weakly magnetic iron minerals. To enrich the strongly magnetic component of the samples (magnetite), the field induction in the mineral separation zone must be in the range

https://doi.org/10.1021/acsomega.1c00129
ACS Omega 2021, 6, 9077−9085

Table 5. Distribution by the Quality of Intergrowths

mineral content in intergrowths (wt %)	there is no mineral	inclusion	bare intergrowths			run-of-mine intergrowths			bucked intergrowths			released grains
	0%	0% < 10%	10% < 20%	20% < 30%	30% < 40%	40% < 50%	50% < 60%	60% < 70%	70% < 80%	80% < 90%	90% < 100%	100%
particle distribution, %	**8.98**	**71.20**	9.76	5.14	2.57	0.43	0.31	0.20	0.13	0.14	0.16	**0.98**
				14.90			**3.51**			**0.43**		
mineral distribution, %	**0**	**24.05**	19.35	17.73	12.56	2.79	2.40	1.89	1.40	1.71	2.14	**13.98**
				37.08			**19.64**			**5.25**		
quartz content in intergrowths, %	**59.30**	**34.33**	**36.83**	**40.27**	**31.09**	**20.56**	**15.77**	**8.87**	**5.87**	**4.24**	**0.99**	**0**
hematite content in intergrowths, %	**23.68**	**43.57**	**34.95**	**23.34**	**27.23**	**23.96**	**21.50**	**17.31**	**12.54**	**5.63**	**2.41**	**0**
magnetite content in intergrowths, %	**4.79**	**15.36**	**11.69**	**8.90**	**4.77**	**5.16**	**4.17**	**2.90**	**1.82**	**0.61**	**0.18**	**0**
hydrogoethite content in intergrowths, %	**22.58**	**5.99**	**5.73**	**5.35**	**6.30**	**7.63**	**7.83**	**6.15**	**5.91**	**3.42**	**0.61**	**0**

Table 6. Iron Distribution by Mineral According to MLA Data

distribution, %					
hematite	magnetite	hydrogoethite	celadonite	carbonate	other
65.09	22.86	10.17	1.34	0.39	0.15

of 0.1−0.2 T. Given the low specific magnetic susceptibility of hematite, it must be enriched at high values of magnetic induction (1.0−1.2 T). Studies were carried out according to a scheme that included grinding to the size of P_{80} = 96 μm and magnetic separation. The magnetic separation cycle included wet magnetic separation (WMS) with a field induction of 0.18 T on a straight-flow drum magnetic separator in the first stage and high-intensity magnetic separation (HIMS) at an induction of 1.0 T in the second stage. The results of beneficiation are presented in Table 7.

Table 7. Results of Magnetic Beneficiation Experiments

product name	γ, %	β Fe_{tot}, %	β SiO_2, %	ε Fe_{tot}, %
concentrate	66.0	52.9	23.8	85.5
tailings	34.0	17.3	73.2	14.5
feed	100.0	40.8	40.6	100.0

To improve the quality of the product, studies were carried out on concentrate regrinding and cleaning. After the first stage of wet magnetic beneficiation, the combined magnetic products were reground to a size of 95%—45 μm. Wet magnetic beneficiation of the second stage was carried out under the following conditions: WMS with a field induction of 0.09 T on a direct-flow drum magnetic separator and HIMS at an induction of 1.2 T. The results of beneficiation according to the two-stage scheme with regrinding are shown in Table 8.

Table 8. Beneficiation Results

product name	γ, %	β Fe_{tot}, %	β SiO_2, %	ε Fe_{tot}, %
concentrate	52.32	58.50	15.70	75.02
tailings	47.68	21.37	67.93	24.98
feed	100.00	40.80	40.60	100.00

The conducted laboratory research showed an increase in the mass fraction of total iron in the combined concentrates after regrinding the combined magnetic concentrate of the first stage of magnetic beneficiation by 5.6 (58.5%) with a decrease in silicon dioxide by 10.2 (15.7%). Studies on magnetic separation have shown that flotation upgrading is necessary to obtain a concentrate with mass fractions of total iron of 69% and silicon dioxide of less than 2.7%. To select the optimal reagent mode, a series of flotation beneficiation experiments were carried out, including studies of the effect of the type and consumption of collecting agents and depressants and the choice of the optimal flotation scheme.

As a result of the laboratory studies of magnetic and flotation concentrations, a magnetic flotation processing scheme was proposed (Figure 7). Wet magnetic concentration after the first stage of grinding was conducted under the following conditions: WMS with an induction field of 0.18 T and HIMS at an induction of 1.0 T. After the first stage of wet magnetic concentration, the combined magnetic products were ground to a size of P_{80} = 45 μm and fed to the wet magnetic

https://doi.org/10.1021/acsomega.1c00129
ACS Omega 2021, 6, 9077−9085

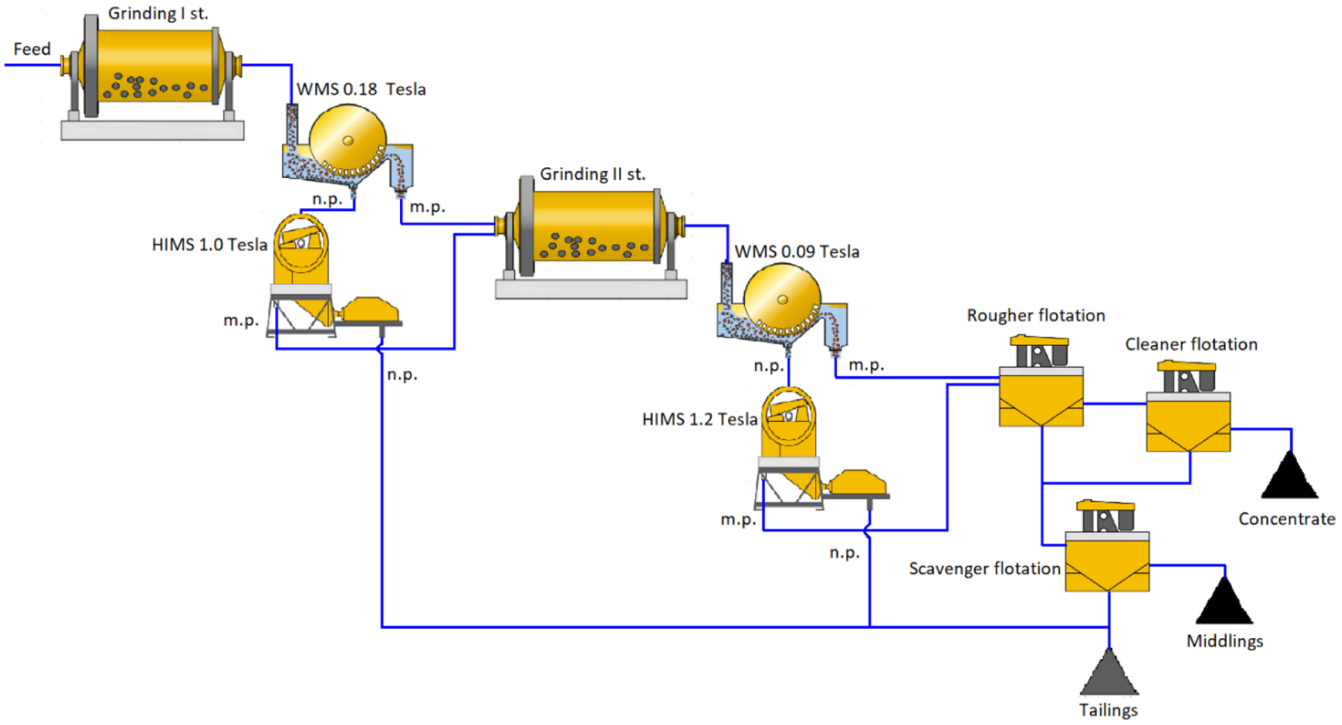

Figure 7. Technological scheme of magnetic flotation.

concentration of the second stage: WMS at a field induction of 0.09 T and HIMS at an induction of 1.2 T.

To achieve the quality of the concentrate (content of total iron is 69%, and silicon dioxide content is less than 2.7%), the refinement of the concentrate was carried out by flotation.[38] Lilaflot from AkzoNobel (Sweden) was used as a collector reagent. Dextrin from Chempack (Russia) was used as a depressor for iron minerals. To create an alkaline environment (pH = 10−10.5), the sodium hydroxide reagent from Chempack (Russia) was used. Dextrin consumption was 250 g/t, and Lilaflot consumption was 180 g/t.

The results of beneficiation according to the magnetic flotation scheme are presented in Table 9, where γ is the yield of the product, β is the content of the component in the product, and ε is the recovery of the component in the product.

Table 9. Results of Beneficiation of Magnetite−Hematite Ores

product name	γ, %	β Fe_{tot}, %	β SiO_2, %	ε Fe_{tot}, %
concentrate	**31.46**	**69.20**	**1.98**	**53.35**
middlings	7.18	62.10	5.51	10.94
tailings	61.36	23.74	64.49	35.71

CONCLUSIONS

As a result of the experimental and theoretical studies, the features of the magnetite−hematite ores of the Mikhailovskoye deposit, which affect the choice of the technology for their beneficiation, were revealed. Analysis of the results of studying the material composition, including chemical composition with an assessment of the content of the main valuable (total iron and magnetite iron) and harmful (silicon oxide, sulfur, and phosphorus) components, granulometric analysis with an assessment of the distribution of iron and silicon oxides by size classes, and features of the mineral composition (textural and structural characteristics, the presence and nature of intergrowths of the ore and rock-forming minerals according to the size classes in the original ore samples, the size of the minerals, and the chemical composition of the iron-containing mineral phases), allows classifying these ores as being very difficult to beneficiate. These types of ores should not be beneficiated using the traditional technological magnetic schemes.

Based on the research results, the technological scheme of magnetic separation followed with flotation was proposed. Iron concentrates with a mass fraction of total iron of 69% and silicon dioxide of less than 2.7% was obtained to produce pellets for subsequent metallization.

MATERIALS

Magnetite−hematite ore of the Mikhailovskoye deposit (Russia) was chosen as the object of research. The Mikhailovskoye deposit is located in the Kursk region of Central Russia and has unique reserves of iron ore. The iron ore stratum belongs to the Proterozoic ferruginous−siliceous−shale formation of the lower Karelia (Kursk type).[36] The Early Proterozoic iron ore strata that is composed of the object underwent regional metamorphism of the greenschist facies,[37,38] which resulted in the formation of the main mineral parageneses. This deposit is located on the western flank of the Mikhailovskaya graben-syncline, and its folded structure is complicated by elements of fracture tectonics, mainly of the folded nature. Iron ores are represented by unoxidized ferruginous quartzites (magnetite, hematite−magnetite, and magnetite−hematite), as well as products of oxidation zones and ancient weathering crusts (oxidized hematite quartzites and rich hematite−martite ores).

The sample was represented by the bulk material (Figure 8) with a size of 70 + 0 mm, and the total sample weight was 40

https://doi.org/10.1021/acsomega.1c00129
ACS Omega 2021, 6, 9077−9085

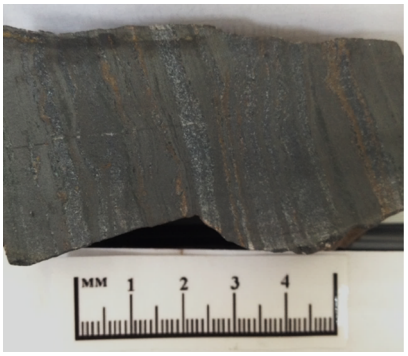

Figure 8. Assay sample of ferruginous quartzite.

kg. Sample preparation for research included crushing operations to a size of 2 mm with further mixing, averaging, and quartering and subsequent sampling of representative samples for chemical and granulometric analyses and mineralogical and technological researches. Experimental studies were conducted at least three times to obtain representative data and error reduction.

EXPERIMENTAL METHODS

Chemical and Mineralogical Analysis. Optical studies were carried out using an ECLIPSE LV100-POL polarizing microscope, an SMZ-1500 optical stereomicroscope equipped with a DS-5M-L1 digital photomicrographic system, and an SMZ-645 stereo microscope. Studies of the mineral composition of the polished minerals section by automated MLA were carried out on a hardware−software complex of the automatic MLA system Quanta 650 (FEI Company, USA). The complex consists of an electron scanning microscope (Quanta 650), two EDAX Silicon Drift Detectors controlled by Genesis software, and integrated MLA Suite software.

To analyze the distribution of iron by valence states in iron ore minerals and gangue minerals, the method of Mossbauer spectroscopy was used. Mossbauer spectra were recorded on an MS-1104Em spectrometer with a Co^{57} source in a rhodium matrix.[34] The isomeric shift was determined relative to α-Fe.

Complete chemical analysis of the samples conducted by energy dispersive X-ray fluorescence spectroscopy (Shimadzu EDX-7000). The resolution under optimal analysis conditions is 125 eV at the 5.89 keV line. Primary X-rays from the X-ray tube excite the sample, producing unique X-rays for the given elements (CaO, P_2O_5, SO_3, SiO_2, Fe_2O_3, Al_2O_3, etc.), which are detected by the unit.

Experimental Research. Experimental studies on the preparation and beneficiation of iron ores were carried out in the laboratories of Saint Petersburg Mining University (jaw crusher, roller crusher, ball mill, Laarmann Flotation Bench Test Machine, laser diffractometer "Mastersaizer" drum magnetic separator BS-20/10-N −12.023, drum magnetic separator PBM-P-25-10, and high-gradient magnetic separator SLON-100). The experimental data were processed using the STATISTICA computer program. Flotation studies: solid content—35%, flotation machine chamber volume—1 L, rotor speed—900 rpm, and airflow rate—1 L/min.

AUTHOR INFORMATION

Corresponding Author

Nadezhda V. Nikolaeva − *Saint Petersburg Mining University, St. Petersburg 199106, Russia;* orcid.org/0000-0001-7492-1847; Email: Nikolaeva_NV@pers.spmi.ru

Authors

Tatiana N. Aleksandrova − *Saint Petersburg Mining University, St. Petersburg 199106, Russia*

Elena L. Chanturiya − *National Research Technological University "MISiS", Moscow 125009, Russia*

Anastasia Afanasova − *Saint Petersburg Mining University, St. Petersburg 199106, Russia*

Complete contact information is available at: https://pubs.acs.org/10.1021/acsomega.1c00129

Notes

The authors declare no competing financial interest.

REFERENCES

(1) Varichev, A. V.; Kretov, S. I.; Kuzin, V. F. *Large-Scale Iron Ore Production*; Gornaya Kniga; MGGU: Moscow, 2010.

(2) Sun, Y.; Zhu, X.; Han, Y.; Li, Y. Green magnetization roasting technology for refractory iron ore using siderite as a reductant. *J. Clean. Prod.* **2019**, *206*, 40−50.

(3) Rath, S. S.; Dhawan, N.; Rao, D. S.; Das, B.; Mishra, B. K. Beneficiation studies of a difficult to treat iron ore using conventional and microwave roasting. *Powder Technol.* **2016**, *301*, 1016−1024.

(4) Das, B.; Mishra, B. K.; Prakash, S.; Das, S. K.; Reddy, P. S. R.; Angadi, S. I. Magnetic and flotation studies of banded hematite quartzite (BHQ) ore for the production of pellet grade concentrate. *Int. J. Miner., Metall. Mater.* **2010**, *17*, 675−682.

(5) Litvinenko, V. S. State policy of Russia in the field of mineral raw materials and legislative support of mining relations. *J. Min. Inst.* **2005**, *166*, 8−10.

(6) Litvinenko, V. S. Digital economy as a factor in the technological development of the mineral sector. *Nat. Resour. Res.* **2020**, *29*, 1521−1541.

(7) Das, S. K.; Das, B.; Sakthivel, R.; Mishra, B. K. Mineralogy, microstructure, and chemical composition of goethites in some iron ore deposits of Orissa, India. *Miner. Process. Extr. Metall. Rev.* **2010**, *31*, 97−110.

(8) Trushko, V. L.; Dashko, R. E.; Kuskov, V. B.; Kornev, A. V.; Klyamko, A. S. Preparation of iron ore raw materials for metallurgical processing. *J. Min. Inst.* **2011**, *194*, 120−123.

(9) Tripathy, S. K.; Singh, V.; Rama Murthy, Y.; Banerjee, P. K.; Suresh, N. Influence of process parameters of dry high intensity magnetic separators on separation of hematite. *Int. J. Miner. Process.* **2017**, *160*, 16−31.

(10) Lvov, V. V.; Kuskov, V. B. A treatability study of the bakcharskoye deposit iron ores concentration by means of high-intensity magnetic separation. *Obogashch. Rud* **2015**, *1*, 26−30.

(11) Ushakov, E.; Aleksandrova, T.; Romashev, A. Neural network modeling methods in the analysis of the processing plant's indicators. *International Scientific Conference on Energy Management of Municipal Facilities and Sustainable Energy Technologies*, 2021.

(12) Romashev, A. O. Use of additive technologies to optimize design of classifying devices. *IOP Conf. Ser.: Mater. Sci. Eng.* **2019**, *665*, 012009.

(13) Kawalla, R.; Brichkin, V. N.; Bazhin, V. Y.; Litvinova, T. E. Ways of rare earth application for iron and steel production technologies. *Innovation-Based Development of the Mineral Resources Sector: Challenges and Prospects—11th Conference of the Russian-German Raw Materials*, 2018, pp 359−365.

(14) Sizyakov, V. M.; Konovalov, G. V.; Konovalov, G. V. Space-oriented unsubmerged streams as a basis of new autogenous apparatus design. *Tsvetnye Met.* **2016**, *10*, 14−20.

(15) Sizyakov, V. M.; Vlasov, A. A.; Vlasov, A. A.; Bazhin, V. Y. Strategy tasks of the russian metallurgical complex. *Tsvetnye Met.* **2016**, *1*, 32−37.
(16) Tsvetkova, A. Y. Review of the main risks of enterprises of the mining and metallurgical industries in modern conditions. *J. Min. Inst.* **2011**, *194*, 339−343.
(17) Donskoi, E.; Poliakov, A.; Holmes, R.; Suthers, S.; Ware, N.; Manuel, J.; Clout, J. Iron ore textural information is the key for prediction of downstream process performance. *Miner. Eng.* **2016**, *86*, 10−23.
(18) Klyamko, A. S.; Trushko, V. L.; Kuskov, V. B. Increasing the competitiveness of iron ore products based on the integrated use of mineral raw materials. *J. Min. Inst.* **2012**, *197*, 245−249.
(19) Ismagilov, R. I.; Baskaev, P. M.; Baskaev, P. M.; Ignatova, T. V.; Shelepov, E. V. The prospects for expanding the iron ore mineral and raw material base through the processing of oxidized ferruginous quartzite of the mikhailovskoe deposit. *Obogashch. Rud* **2020**, *3*, 19−24.
(20) Yuan, S.; Zhou, W.; Han, Y.; Li, Y. Selective enrichment of iron particles from complex refractory hematite-goethite ore by coal-based reduction and magnetic separation. *Powder Technol.* **2020**, *367*, 305−316.
(21) Kondrasheva, N. K.; Rudko, V. A.; Kondrashev, D. O.; Gabdulkhakov, R. R.; Derkunskii, I. O.; Konoplin, R. R. Effect of delayed coking pressure on the yield and quality of middle and heavy distillates used as components of environmentally friendly marine fuels. *Energy Fuels* **2018**, *33*, 636−644.
(22) Zhang, X.; Gu, X.; Han, Y.; Parra-Álvarez, N.; Claremboux, V.; Kawatra, S. K. Flotation of iron ores: A review. *Miner. Process. Extr. Metall. Rev.* **2019**, *42*, 184−212.
(23) Turrer, H. D. G.; Peres, A. E. C. Investigation on alternative depressants for iron ore flotation. *Miner. Eng.* **2010**, *23*, 1066−1069.
(24) Liu, Q.; Wannas, D.; Peng, Y. Exploiting the dual functions of polymer depressants in fine particle flotation. *Int. J. Miner. Process.* **2006**, *80*, 244−254.
(25) Pavlovic, S.; Brandão, P. R. G. Adsorption of starch, amylose, amylopectin and glucose monomer and their effect on the flotation of hematite and quartz. *Miner. Eng.* **2003**, *16*, 1117−1122.
(26) Araujo, A. C.; Viana, P. R. M.; Peres, A. E. C. Reagents in iron ores flotation. *Miner. Eng.* **2005**, *18*, 219−224.
(27) Ma, X.; Marques, M.; Gontijo, C. Comparative studies of reverse cationic/anionic flotation of Vale iron ore. *Int. J. Miner. Process.* **2011**, *100*, 179−183.
(28) Trushko, V. L.; Utkov, V. A.; Utkov, V. A.; Klyamko, A. S. Increasing gas-permeability of sinter mix with high content of finely-ground iron ore concentrate. *Obogashch. Rud* **2015**, *3*, 32−34.
(29) França, J. R. O.; Barrios, G. K. P.; Turrer, H. D. G.; Tavares, L. M. Comminution and liberation response of iron ore types in a low-grade deposit. *Miner. Eng.* **2020**, *158*, 106590.
(30) Singh, S.; Sahoo, H.; Rath, S. S.; Palei, B. B.; Das, B. Separation of hematite from banded hematite jasper (BHJ) by magnetic coating. *J. Cent. S. Univ.* **2015**, *22*, 437−444.
(31) Zhang, Q.; Zhao, X.; Lu, H.; Ni, T.; Li, Y. Waste energy recovery and energy efficiency improvement in China's iron and steel industry. *Appl. Energy* **2017**, *191*, 502−520.
(32) Reichert, M.; Gerold, C.; Fredriksson, A.; Adolfsson, G.; Lieberwirth, H. Research of iron ore grinding in a vertical-roller-mill. *Miner. Eng.* **2015**, *73*, 109−115.
(33) da Costa, G. M.; Barrón, V.; Mendonça Ferreira, C.; Torrent, J. The use of diffuse reflectance spectroscopy for the characterization of iron ores. *Miner. Eng.* **2009**, *22*, 1245−1250.
(34) Batisteli, G. M. B.; Peres, A. E. C. Residual amine in iron ore flotation. *Miner. Eng.* **2008**, *21*, 873−876.
(35) Filippov, L.; Filippova, I. V.; Severov, V. V. New technology for production of hematite concentrate from current tailings of ferrous quartzite processing. *Metallurgist* **2010**, *54*, 268−272.
(36) *Iron Ores from KMA*; Orlov, V. P.; Shevyreva, I. A.; Sokolova, N. A., Eds.; CJSC "Geoinformmark", 2001.
(37) Zhdanov, V. V. Iron-ore skarns and ferruginous quartzites. *Otechestvennaya Geol.* **1993**, *4*, 25−32.
(38) Zhdanov, V.; Belyaev, G.; Bluman, B.; Vishnevskaya, Y.; Maslov, A.; Kuzmin, V.; Petrov, B. N. *Regional Metamorpho-Metasomatic Formations*; Elsevier, 1983.

https://doi.org/10.1021/acsomega.1c00129
ACS Omega 2021, 6, 9077−9085